Isothermal Adsorption of Aflatoxin B_1 on HSCAS Clay

Patrick G. Grant and Timothy D. Phillips*

Intercollegiate Faculty of Toxicology, College of Veterinary Medicine, Texas A&M University, College Station, Texas 77843-4458

Previously, hydrated sodium calcium aluminosilicate (HSCAS), a phyllosilicate clay of the smectite class, was shown to tightly bind aflatoxins and prevent aflatoxicosis in animals. HSCAS is a commercial feed additive that is approved to be used as an anticaking agent. In this study, aflatoxin B_1 (AfB_1) was isothermally mixed with HSCAS at 15, 25, and 37 °C to study the adsorption process. An L adsorption isotherm was characterized from the data, which were fitted to multiple isotherm equations (i.e., Langmuir, multi-Langmuir, general Freundlich, Langmuir−Freundlich combination, Toth, and various transforms of these equations). Information derived from the isotherm equations included capacity, affinity, average capacity, enthalpy of binding, heterogeneity coefficient, multiple site distribution coefficients, and a multisite capacity. Physical characteristics of AfB_1 and HSCAS were measured and modeled to further the understanding of the adsorption process. The data obtained support the hypothesis that AfB_1 chemisorbs to different sites on HSCAS which could include the interlamellar region, edges, and basal surfaces of HSCAS particles.

Keywords: *Adsorption; aflatoxin; binding; clay; detoxification; HSCAS; isotherm; smectite*

INTRODUCTION

Aflatoxins are a group of pervasive, secondary fungal metabolites produced by *Aspergillus flavus* and *parasiticus* molds. Concern about aflatoxins originate from strong implications of its involvement in disease and death in humans and animals. Aflatoxin B_1 (AfB_1) (Figure 1) is the most acutely toxic (Carnaghan et al., 1963) and hepatocarcinogenic (Wogan and Newberne, 1967) of the 16 naturally occurring aflatoxins. Aflatoxins B_1, B_2, G_1, and G_2 are the most commonly detected aflatoxins in a variety of foods and feedstuffs (CAST, 1989).

Every year a significant percentage of the world's grain and oilseed supply is contaminated with aflatoxins (CAST, 1989). This contamination results in the discarding of tainted foodstuffs in countries with an abundance of resources and the consumption of contaminated foodstuffs in countries with limited resources for both humans and livestock. Dairy animals can also secrete carcinogenic metabolites (aflatoxin M series) in their milk following the ingestion of aflatoxin-contaminated feed (Allcroft and Carnaghan, 1963). Since aflatoxin compounds are either known human carcinogens or suspected carcinogens, complete avoidance would be the best situation. Detection and quantification of aflatoxins before food processing are difficult because of the heterogeneous distribution of mold contamination. The majority of a feed may be below the action level of 20 ppb (CAST, 1989), but a small portion could contain much higher levels. After processing and mixing, an entire load could be below the regulatory action level concentration, but not free from aflatoxins. The ubiquitous nature and the harmful effects caused by aflatoxin contamination require practical and effective strategies to detoxify and remediate contaminated food and feed.

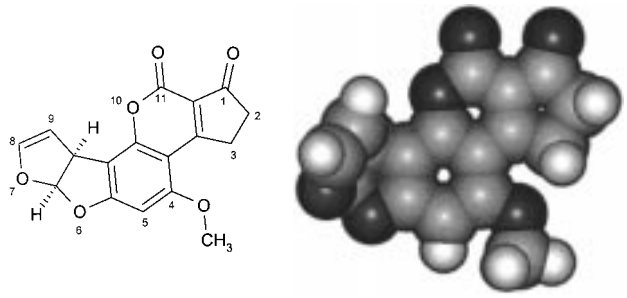

Figure 1. Structure of AfB_1 (left) and the molecular model (right) illustrating the spatial orientation and size of the functional groups.

Previous in vitro studies have shown that hydrated sodium calcium aluminosilicate (HSCAS) in aqueous solutions binds AfB_1 and analogues of AfB_1 containing the β-dicarbonyl system (Phillips et al., 1988; Sarr, 1992). This anticaking commercial feed additive (NovaSil) has been reported to protect multiple animal species from the deleterious effects of this group of toxins (Phillips et al., 1995). HSCAS, a smectite clay, has also been shown to reduce the production of aflatoxin M_1 that contaminates the milk of lactating animals (Harvey et al., 1991; Smith et al., 1994). The protection from aflatoxin contamination occurs when as little as 0.5% HSCAS is added to the diet of the animal species (Phillips et al., 1995). The protection results from the adsorption of aflatoxins to HSCAS in the gastrointestinal tract, thus reducing the bioavailability of the aflatoxins. However, the adsorption mechanism of AfB_1 to HSCAS is not fully characterized.

One of the most efficient ways of investigating surface adsorption is through the use of isotherms. Multiple isotherm equations have been proposed for the modeling of the adsorption of compounds in aqueous solutions to

* Author to whom correspondence should be addressed [telephone (409) 845-3517; fax (409) 862-4929; e-mail tphillips@cvm.tamu.edu].

S0021-8561(97)00604-3 CCC: $15.00
Published on Web 01/14/1998

Table 1. Isotherm Equations Used To Fit Plots of AfB_1 Binding to HSCAS Clay[a]

Eadie−Hofstee (EHT)	$q = Q_{max} - (1/K_d)(q/C_w)$
Langmuir model (LM)	$q = Q_{max}\left(\frac{K_d C_w}{1 + K_d C_w}\right)$
Langmuir−Freundlich model (LFM)	$q = Q_{max}\left(\frac{(K_d C_w)^n}{1 + (K_d C_w)^n}\right)$
Lineweaver−Burk transform (LBT)	$1/q = 1/Q_{max} + (1/(K_d Q_{max})(1/C_w))$
generalized Freundlich model (GFM)	$q = Q_{max}\left(\frac{(K_d C_w)}{1 + (K_d C_w)}\right)^n$
reciprocal Langmuir transform (RLT)	$C_w/q = (1/(K_d Q_{max}) + (1/Q_{max})C_w)$
Scatchard transform (ST)	$q/C_w = K_d Q_{max} - K_d q$
Toth model (TM)	$q = Q_{max}\left(\frac{(K_d C_w)}{(1 + (K_d C_w)^n)^{1/n}}\right)$

[a] q = concentration of AfB_1 adsorbed (mol/kg), Q_{max} = maximum capacity (mol/kg), K_d = distribution constant, C_w = equilibrium concentration of AfB_1. LM, LFM, GFM, and TM plots were fitted with q vs C_w while EHT was fitted with q vs q/C_w, LBT with $1/q$ vs $1/C_w$, RLT with C_w/q vs C_w, and ST with q/C_w vs q.

the surfaces of solids (Kinniburgh, 1986). These equations contain similar variables and differ mainly in the arrangement of the variables (Table 1). The Langmuir equation is most applicable to a single ligand adsorbing to a single type of site on a particular sorbent (Langmuir, 1916). The Langmuir equation has both a capacity (Q_{max}) and an affinity (K_d) parameter; the Toth equation contains these parameters, as well as an exponent (n) that represents the heterogeneity of the adsorption (Kinniburgh, 1986). The Langmuir−Freundlich, generalized Freundlich, and Toth equations are applicable to heterogeneous solid surfaces. Several mathematical transforms have been derived: the Eadie−Hofstee (EHT), Lineweaver−Burk (LBT), Scatchard (ST), and reciprocal Langmuir (RLT) can be used to estimate Q_{max} and K_d of adsorption. Heterogeneous adsorption could be modeled by the addition of Langmuir equations representing different sites (Langmuir, 1916). This summation of Langmuir isotherm equations (MLM) was recently investigated (Cernik et al., 1995). Isotherm shapes are categorized into four types of curves, designated H, L, C, and S, which represent different adsorption mechanisms (Giles et al., 1960, 1974a,b).

The Gibbs standard free energy change of adsorption ($\Delta G°_{ads}$) and the enthalpy of adsorption (ΔH_{ads}), which can be calculated from the K_d values (Fischer and Peters, 1970; Stumm et al., 1992), give information on the mechanism of adsorption. In particular, the adsorption of compounds to a surface can be categorized as either physisorption or chemisorption on the basis of ΔH_{ads} (Gatta, 1985). Physisorption involves weak associations which include van der Waals, dipole−dipole, induced dipole, and hydrogen bonding. Chemisorption implies a chemical reaction or sharing of electrons between the adsorbent and the adsorbate. Physisorption is described as having an enthalpy of <20 kJ/mol, while chemisorption is generally >20 kJ/mol (Gu et al., 1994).

The objectives of this study were to (1) determine various physical characteristics of AfB_1 and HSCAS and (2) use isotherms to measure the capacity, number of sites, strength, and thermodynamics of AfB_1 adsorption on HSCAS.

MATERIALS AND METHODS

Chemical Reagents. AfB_1 was purchased from Sigma Chemical Co. (St. Louis, MO). HSCAS (NovaSil) was obtained from Engelhard Corp. (Cleveland, OH) and was sieved to ≤45 μm particle size. Collapsed HSCAS (Col-HSCAS) was prepared by heating HSCAS to 200 °C for 30 min and then heating the sample at 800 °C for 1 h. All solvents were HPLC grade (Burdick and Jackson, Muskegon, MI). The water used in these studies was prepared by processing deionized water through a Milli-Q^{uf+} system.

Aflatoxin Characteristics. The octanol water partition coefficient (K_{ow}) of AfB_1 was estimated by two methods. The first method began with the construction of a two-dimensional structure of AfB_1 in ISIS Draw 2.0 (MDL Information Systems, San Leandro, CA), which was then imported it into HyperChem 4.5 (HyperCube, Ontario, Canada) to create a three-dimensional structure. The model of AfB_1 was energy minimized using the semiempirical quantum mechanical AM1 method (Dewar et al., 1985; HyperChem, 1994). The structural information was then imported to a ChemPlus module for the determination of log K_{ow}. ChemPlus utilizes previously derived atomic parameters to estimate each individual atom's contribution to the log K_{ow} (ChemPlus, 1993; Ghose et al., 1988; Vellarkad et al., 1989).

The K_{ow} was also measured with an established HPLC method based on comparing the capacity factor (k') of the unknown to the k' of a training set of compounds with known K_{ow} values. The method used a 3:1 mobile phase of methanol to water (Klein et al., 1988). The compounds selected for the training set were benzene, benzophenone, benzyl alcohol, phenol, and, toluene. The unretained compound was a 1 mM solution of $Ca(NO_3)_2$. The chromatographic capacity factor (k') for each standard was determined by subtracting the time of detection of the unretained compound from the retention time of the standard and dividing by the detection time of the unretained compound $\{(t_c - t_r)/t_r\}$. The published log K_{ow} was plotted versus the k' found for the training set of compounds on this HPLC system. A linear regression was done on the data points to obtain an equation for log K_{ow} from the k' value. The k' for AfB_1 was placed in this equation to get a value for the K_{ow} of AfB_1.

Previous research has determined a correlation among the K_{ow}, melting point (mp), molecular weight (MW), and solubility (S) of organic molecules (Meylan et al., 1996). The measured K_{ow}, along with the mp and MW, was used to estimate the solubility of AfB_1 by entering these data values into the correlation equation given below.

$$\log S = 0.693 - 0.96K_{ow} - 0.0092(\text{mp} - 25) - 0.00314(\text{MW})$$

The AfB_1 structure in ChemPlus was also used to measure the cross-sectional area of the molecule. The van der Waals radii of C, O, and H were set to 1.85, 1.40, and 1.20 Å, respectively (Emsley, 1991). The structure of AfB_1 was oriented on edge with the dicarbonyl in view and planar with the dihydrofuran in view. The cross-sectional area method was modified by the use of a carbon atom as the reference for the area calculations (Gray et al., 1995).

HSCAS Characteristics. The total organic carbon (TOC) in HSCAS was determined using a Leco model 523-300 induction furnace. The sample was previously acidified with 10% hydrochloric acid to remove any inorganic carbon which exists as carbonates. Organic carbon was then converted into

CO_2 and was measured with a Horiba IR detector with the signal being integrated by a Hewlett-Packard 3369a integrator.

The concentration of 38 elements in HSCAS was measured by neutron activation. The external surface area of HSCAS was measured by N_2 adsorption. The sample preparation consisted of heating the clay at 125 °C for 12 h. The data of adsorption and desorption isotherms were fit to the BET isotherm equation (Adamson, 1982).

The total surface areas of HSCAS and Col-HSCAS were determined by measuring the amount of ethylene glycol adsorbed onto the clay (Mortland and Kemper, 1965). The surface area was calculated on the basis of the relationship that 3.1×10^{-5} g of ethylene glycol covers each square meter of surface (Dyal and Hendricks, 1950).

Isothermal Adsorption. A stock solution of AfB_1 was prepared by dissolving the pure crystals in acetonitrile. A volume of the stock solution was then injected into purified water, yielding an 8 μg/mL solution of AfB_1. The working solution's concentration was then checked with the UV−vis spectrophotometer. The batch isotherm procedure entailed the exposure of samples containing 50 μg of HSCAS or Col-HSCAS to an increasing concentration of solute (0.4, 0.8, 1.6, 2.4, 3.2, 4, 4.8, 6, 6.4, 7.2, and 8 μg/mL). This study used three replicates at each solute concentration. The solute concentration was achieved by adding an appropriate amount of working solution to sterile 17 × 100 mm polypropylene centrifuge test tubes and then adding the complementary amount of purified water to make the total volume 5 mL. Approximately 5 mg of sorbent was weighed in a 16 × 125 mm disposable borosilicate test tube, and purified water was added to the sorbent to make a 1 mg/mL suspension. The sorbent/water suspension was vortexed for 3 s before each 50 μL transfer to each replicate by an autopipetter. The mixing was repeated before each transfer. Along with the samples, there were three controls consisting of 5 mL of purified water, 5 mL of stock solution without sorbent, and 5 mL of the lowest concentration without sorbent. The samples and controls were capped and placed on an electric shaker at 1000 rpm for 24 h in an incubator at either 15, 25, or 37 °C. After shaking, the samples were centrifuged at 10 000 rpm for 15 min at the same temperature that the shaking occurred. The UV−vis absorption of the supernatant from the samples and controls was measured with the spectrometer. At the highest concentration level, the supernatant was saved for analysis by HPLC to check for any degradation compounds because the adsorption calculations are dependent on a difference calculation.

Data Calculations and Curve Fitting. The UV−vis absorption data were used to calculate the amount of AfB_1 left in solution and amount adsorbed for each data point. These data were then used to fit isotherm equations to obtain values for the variable parameters. The isotherm equations (Table 1) were entered as user-defined functions. Each function has limits and beginning values or first approximations for the variable parameters. The parameter limits for Q_{max} were positive numbers ranging from 0 to a maximum of 1 kg/kg. The parameter limits for K_d were from 0 to 1×10^{25}. The parameter range for n was from 0 to 1. Estimates for the Q_{max} and K_d were taken from the double-logarithmic plot of the isotherm (Figure 2) (Stumm et al., 1992). The plot will normally display a break in the curve. The value on the x axis where the curve breaks is an estimate of K_d^{-1}. The value on the y axis where the curve breaks is an estimate of Q_{max}. These values for the ranges and estimates were entered into the user-defined functions.

The fitting of MLM to the data enables the estimation of the number of different types of sites on the sorbent, the strength of binding, and the capacity of the sites. User-defined equations were used to represent the linear addition of one to six Langmuir equations. The method employed used constraints in the fit of the multiple Langmuir to overcome the difficulty of an ill-posed mathematical problem. The constraints in fitting the data are to limit the site capacity and the distribution coefficient to positive values. These equations were fit to the data and listed by decreasing r^2. The variable parameters were set to values as previously described. The

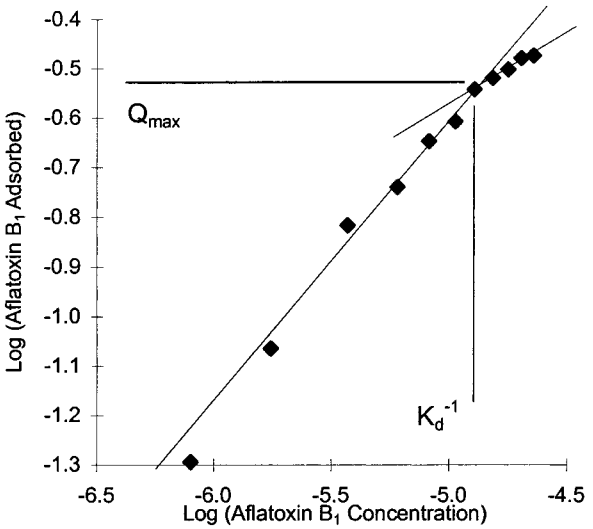

Figure 2. Log−log plot of the isothermal adsorption of AfB_1 to HSCAS for estimation of Q_{max} and K_d.

Table 2. Thermodynamic Equations Used with Adsorption Parameters

$$\Delta G° = -RT \ln K_d \quad (1)$$

$$\Delta H_{ads} = \frac{-R \ln(K_{d2}/K_{d1})}{(1/T_2) - (1/T_1)} \quad (2)$$

Table 3. Measured Physical Characteristics of AfB_1, HSCAS, and Col-HSCAS

AfB_1	
log K_{ow}	1.46 and 1.98
solubility	11−33 μg/mL
ϵ	21865 (1/(M(cm))
vertical cross-sectional area	52.8 Å^2
horizontal cross-sectional area	88.3 Å^2
HSCAS	
total surface area	848 m^2/g
external surface area	70 m^2/g
total organic carbon	<0.05%
Primary Metals	
aluminum	8%
calcium	1.74%
iron	2.22%
magnesium	0.5%
Col-HSCAS	
total surface area	77 m^2/g

equations that fit the data with the best r^2 were judged on the randomness of the residuals. The equation that represent the lowest number of Langmuir equations, satisfied a high r^2, and had a random residual plot was selected as an estimate of both the adsorption process and the number of sites. From the fitting of these equations, the Q_{max} and K_d were found for each site.

The enthalpy was calculated by comparing the individual K_d values at 15, 25, and 37 °C by eq 2 (Table 2). The definition of K_d is derived by solving for K_d from the Langmuir equation (Table 1) giving

$$K_d = q/(Q_{max} - q)C_w$$

The Q_{max} is taken from the fit of LM to the adsorption data at 15, 25, and 37 °C.

Statistics. Samples used for isotherms and surface area adsorption experiments were done in triplicate in order to calculate a standard deviation for each sample level. Statistically significant difference analysis was done on the log−log

regression isotherm plots of HSCAS and Col-HSCAS using the GB-Stat analysis program. The statistical hypotheses of a common regression line and a common slope between the plots were tested.

RESULTS AND DISCUSSION

The molecular model estimate and HPLC measurement of the log K_{ow} of AfB_1 were 1.456 and 1.98, respectively (Table 3). The literature value for the solubility of AfB_1 in water has varied from 10 to 30 μg/mL (Busby and Wogan, 1984). The results of the solubility estimate using the equations published by Meylan et al. (1996) gave a similar range of 11−33 μg/mL solubility (Table 3). This estimate in solubility was used to set the maximum solution concentration in these studies to 8 μg/mL to ensure that precipitation would not be a factor.

AfB_1 is hydrophobic and slightly soluble in water as shown by the K_{ow} and the solubility range. This would suggest that AfB_1 would partition well to organic constituents in the clay. However, the TOC of HSCAS is <0.05%, which demonstrates that there is essentially no organic material previously adsorbed to the clay. In previous studies the binding of aflatoxin analogues to HSCAS was dependent upon an intact β-dicarbonyl system (Sarr, 1992). This specificity of the binding and the lack of organic carbon in HSCAS confirm that the organic partitioning mechanism is not substantial in the adsorption of AfB_1 and therefore the protection of animals from aflatoxicosis by HSCAS.

HSCAS was found to have a high total surface area of 848 ± 11 m^2/g by the ethylene glycol adsorption method (Table 3). This high surface area value is typical of the smectite series of clay. Smectite clays have a large internal surface area that can be as high as 800 m^2/g (Borchardt, 1989). Surface area measurements by N_2 adsorption measure the external surface area of clay minerals. The external surface area of HSCAS was measured by the N_2 and was implied by the measurement of Col-HSCAS with ethylene glycol adsorption and found to be 70 and 77 ± 2 m^2/g, respectively (Table 3). The collapsing of the interlamellar region leaves only the exterior surface available for the ethylene glycol adsorption. The near agreement between these methods confirms the collapse of HSCAS and loss of the interlamellar region for adsorption on Col-HSCAS.

The isotherm shape of AfB_1 adsorption on HSCAS can be categorized as L1 or L2, which represents an L type isotherm plot that is reaching or has reached a plateau, respectively (Figure 3). Whether or not an isotherm plot has reached a plateau can be implied by comparing the Q_{max} of the fitted isotherm equation with the observed maximum adsorbed quantity. The maximum of AfB_1 adsorbed onto HSCAS was 0.336 mol/kg (Table 4), which is 72.9% of the Q_{max} of 0.461 mol/kg (Table 4) from the fitting of the LM to the data. This suggests that a majority of the capacity is occupied by AfB_1, that a plateau is being reached, and that the isotherm plot is an L2.

Specific interactions between the adsorbent and the adsorbate are likely both chemisorption in mechanism and to have an L type isotherm (Adamson, 1982). The initial strong adsorption and then the plateau of the isotherm plot suggest a specific type of binding and the saturation of that type of site. The shape of the isotherm plot of AfB_1 binding to Col-HSCAS was an L2

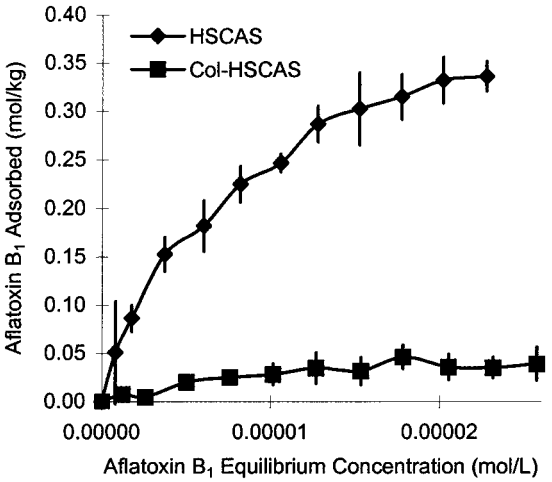

Figure 3. Isotherm plot for AfB_1 adsorption to HSCAS and Col-HSCAS at 25 °C.

type of isotherm plot (Figure 4) that had capacity smaller (0.0567 mol/kg) than untreated HSCAS (0.461 mol/kg), suggesting that a significant portion of the binding of AfB_1 to HSCAS is within the interlamellar region of the clay. The isotherm plots of HSCAS and Col-HSCAS were shown to be statistically different (Figure 5). The test of the statistical hypothesis of a common regression was dismissed since an F ratio of 465 and a chance probability of <0.0001 was calculated. However, the hypothesis test of a common slope was not dismissed because an F ratio of 1.07 and a chance probability of 0.31 were calculated.

The Toth exponent has a range of 0−1 with 1 representing homogeneous sites and with numbers approaching 0 representing more heterogeneous sites. The fitting of the data to the Toth isotherm gave an exponent of 0.64 (Table 4), which indicates more than one type of site binding AfB_1 to HSCAS. The curve fit of the MLM also infers that there are at least two sites. The first site had a distribution constant of 1.44×10^6 and a capacity of 0.041 mol/kg. The second site had a distribution constant of 8.33×10^4 and a capacity of 0.461 mol/kg. The summation of these capacities agrees with the average estimate of the capacity of the isotherm models used (Table 4). The curve fitting of the MLM had an r^2 value of 0.997 but had an unacceptable standard error for the Q_{max} of the minor site. This could be improved by increasing the number of data points. Once the error for the Q_{max} of the minor site is improved, it will be necessary to compare this Q_{max} to the Q_{max} of the Col-HSCAS since they are of the same magnitude. These capacities being similar would agree with the proposal of at least two sites of adsorption to HSCAS with the major site being the interlamellar region. Other transforms and isotherm models were used but did not fit as well (r^2) or have as small of a standard error in the Q_{max} estimate as the LM (Table 4).

The LM was also used to estimate the Q_{max} at different isotherm temperatures to calculate individual K_d values to use in the enthalpy of adsorption calculations. The enthalpy of adsorption plot of AfB_1 binding to HSCAS shows some minor variation which could indicate multiple sites with dissimilar thermodynamic properties (Figure 6). The enthalpy plot indicated that all the sites probably involve a chemisorption mechanism because the enthalpy was near or above −40 kJ/mol. The K_d from the LM was used to show that, from

Table 4. Summary of Isotherm Fit Parameters of AfB_1 Adsorption onto HSCAS

isotherm model	capacity ± std[a] error	K_d	exponent	r^2
average of models and transforms	0.485 ± 0.082	122 000	NA[b]	NA
Langmuir model (LM)	0.461 ± 0.015	121 000	NA	0.9957
Langmuir−Freundlich model (LFM)	0.560 ± 0.070	76 000	0.833	0.9972
generalized Freundlich model (GFM)	0.512 ± 0.035	63 000	0.764	0.9973
multi-Langmuir model (MLM)	0.461 and 0.041	83 300−1 440 000	NA	0.9974
Toth model (TM)	0.650 ± 0.200	129 000	0.640	0.9971
transforms	**capacity ± std error**	**K_d**	**exponent**	**r^2**
Eadie−Hofstee (EHT)	0.413 ± 0.016	160 400	NA	0.9460
Lineweaver−Burk transform (LBT)	0.385 ± 0.026	187 000	NA	0.9927
reciprocal Langmuir transform (RLT)	0.445 ± 0.014	134 500	NA	0.9907
Scatchard transform (ST)	0.438 ± 0.020	144 000	NA	0.9420
experimental data summary	**maximum adsorbed**	**K_d range**		
observed data	0.336 ± 0.015	108 000−155 000	NA	NA

[a] std = standard. [b] NA = not applicable.

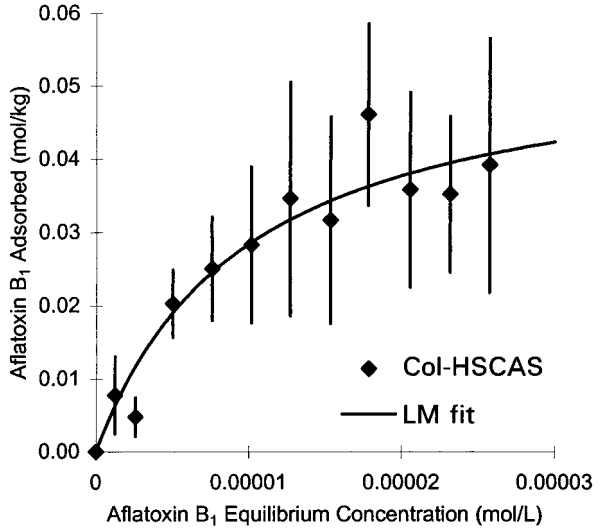

Figure 4. Isotherm plot for AfB_1 adsorption to Col-HSCAS at 25 °C with the data fit to the Langmuir model.

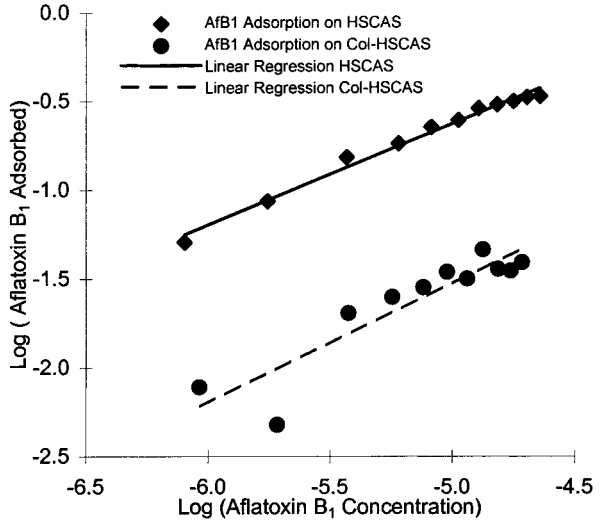

Figure 5. Log−log plot of the isothermal adsorption of AfB_1 to HSCAS and Col-HSCAS for statistical analysis.

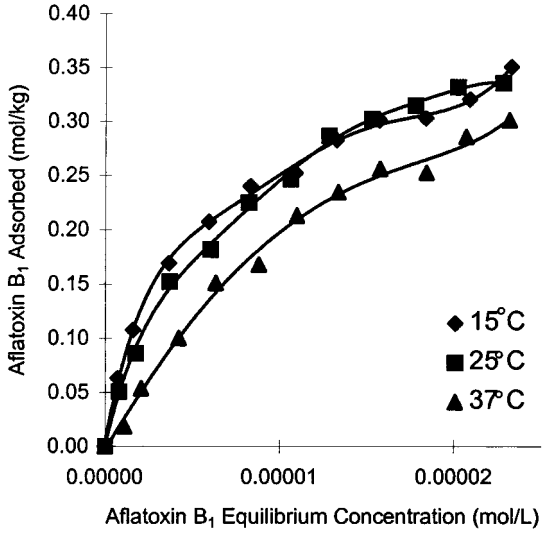

Figure 6. Isotherm plots for AfB_1 adsorption to HSCAS at 15, 25, and 37 °C which were used to calculate the enthalpy of adsorption.

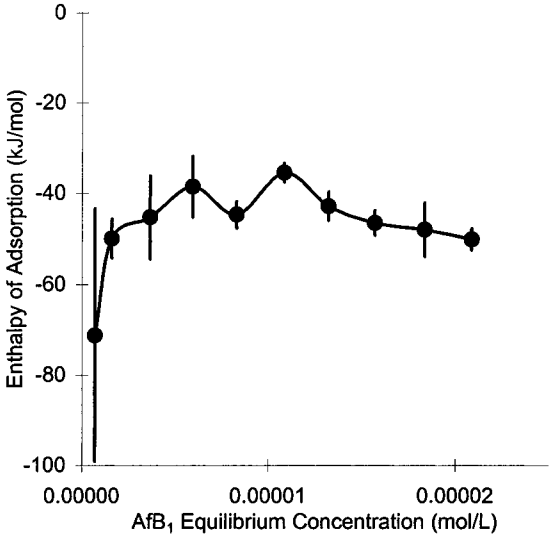

Figure 7. Average enthalpy calculation plot from isothermal adsorption of AfB_1 to HSCAS at 15, 25, and 37 °C.

eq 1 (Table 2), ΔG was negative (−29 kJ/mol), and so the adsorption was spontaneous.

The Q_{max} from the LM was used with the total surface and external surface areas to calculate the amount of coverage of AfB_1 on the clay, the importance of the interlamellar region, and whether a multilayer formation was possible. Both the total surface area and the external surface area of a kilogram of HSCAS were divided by the maximum number of molecules adsorbed by a kilogram of HSCAS. This results in the available surface area per bound AfB_1 molecule. This value was

then compared to the cross-sectional areas of the probable orientations of a bound AfB_1. One of the orientations (vertical) was with the dicarbonyl system bound to the clay, because this moiety was found to be important in previous research (Sarr, 1992). The other orientation (horizontal) was with the molecule lying planar on the surface with the dihydrofuran away from the surface. The vertical and horizontal cross-sectional areas were found to be 52.8 and 88.3 $Å^2$, respectively (Table 3).

The total surface area of HSCAS relative to the bound AfB_1 molecules is 305 $Å^2$/molecule, which could bind the full amount of AfB_1 in either orientation without requiring a multilayer coverage. The outer area of HSCAS relative to the amount of AfB_1 bound is 25.2 $Å^2$/molecule, which is smaller than the area required by either orientation. This would suggest that the interlamellar region is very important to the binding of AfB_1 and that AfB_1 is forming a multilayer on the exterior of the HSCAS particles. The number of layers required for external binding would range between slightly less than two for the vertical orientation and up to three for the horizontal orientation. The multilayer mechanism is normally a weak association and would not be a specific adsorption mechanism. Likewise, the multilayer mechanism would conflict with the enthalpy of adsorption plot, the indicated chemisorption mechanism from the enthalpy plot, the saturation of sites for a L2 isotherm plot, or the lack of binding for the Col-HSCAS. If the external surface was responsible for the entire amount of binding, then the collapse of the clay would have had a minimal effect on the binding.

Previous research compared the DRIFT analysis of HSCAS and HSCAS with AfB_1 adsorbed. The results of that investigation showed the disappearance of the adsorption due to C═O stretching and the appearance of new adsorption bands (Sarr, 1992). The new adsorption bands are within the same region as Cu^{2+}, Pd^{2+}, and Al^{3+}−acetylacetonates (Nakamoto, 1963; Sarr, 1992). Because HSCAS is free from organic constituents and the adsorption is specific, it is thought that AfB_1 binds or reacts with a metal ion or metal surface site. Numerous trace metals are found in HSCAS, but only five are concentrated enough to bind the amount of AfB_1 that is bound to HSCAS. The five major constituents of HSCAS are Al, Ca, Fe, Mg, and Si. The abundance of these elements was determined by neutron activation to be Al at 8%, Ca at 1.74%, Fe at 2.22%, and Mg at 0.5% (Table 3). Metal edge sites made of Al, Fe, Mg, and Si could be responsible for a minor part of the adsorption as indicated by the Col-HSCAS isotherm. Interaction with Ca in the interlamellar region may be responsible for the majority of the adsorption to HSCAS.

HSCAS has previously been shown to protect animals from aflatoxicosis. This protection is attributed to chemisorption within the interlamellar region of the clay with a minor amount being adsorbed on the exterior of the clay. Research will continue to investigate the hypothesis of AfB_1 adsorption to the metal edge sites, interlaminar region, and Ca interactions. Further research will investigate the hypothesis that the positive charge of the carbons of the β-dicarbonyl system is responsible for adsorption through an electron donor acceptor (EDA) mechanism with the surface of the clay. This will be accomplished with molecular modeling and further comparison of clays with various chemical properties.

SAFETY

Aflatoxins are hazardous chemicals and should be handled with extreme care. Protective clothing, gloves, a fume hood, and goggles are critical requirements to prevent aflatoxin exposure. Aflatoxin in the crystalline form can become electrostatically charged and airborne. Aflatoxin solutions and residues on glassware can be decontaminated with a commercially available bleach solution.

ABBREVIATIONS USED

AfB_1, aflatoxin B_1; AfM_1, aflatoxin M_1; DRIFT, diffuse reflectance infrared Fourier transform spectroscopy; HSCAS, hydrated sodium calcium aluminosilicate; k', capacity factor; K_d, distribution coefficient; K_{ow}, octanol water partition coefficient; mp, melting point; MW, molecular weight; NA, not applicable; TOC, total organic carbon

ACKNOWLEDGMENT

We express special thanks to GERG (Geochemical and Environmental Research Group), the Texas A&M Chemical Characterization Center, and Quantachrome Corp. for the TOC, neutron activation, and surface area measurements, respectively.

LITERATURE CITED

Adamson, A. W. The Solid-Liquid Interface Adsorption from Solution. In *Physical Chemistry of Surfaces*, 4th ed.; Wiley: New York, 1982; pp 369−401.

Allcroft, R.; Carnaghan, R. B. A. Groundnut Toxicity: An Examination for Toxins in Human Food Products from Animals Fed Toxic Groundnut Meal. *Vet. Rec.* **1963**, *75*, 259−263.

Borchardt, G. Smectites. In *Minerals in Soil Environments*; Dixon, J. B., Weed, S. B. Eds.; Soil Science Society of America: Madison, WI, 1989; pp 675−727.

Busby, W. F. J.; Wogan, G. N. Aflatoxins. In *Chemical Carcinogens*, 2nd ed.; Searle, C. E., Ed.; American Chemical Society: Washington, DC, 1984; Vol. 2, pp 945−1136.

Carnaghan, R. B. A.; Hartley, R. D.; O'Kelly, J. Toxicity and Fluorescence Properties of the Aflatoxins. *Nature* **1963**, *200*, 1101.

Carter, M. C.; Kilduff, J. E.; Weber, W. J. J. Site Energy Distribution Analysis of Preloaded Adsorbents. *Environ. Sci. Technol.* **1995**, *29*, 1773−1780.

CAST (Council for Agricultural Science and Technology). In *Mycotoxins: Economic and Health Risks*; Task Force Report 116; Niyo, K., Ed.; CAST: Ames, IA, 1989; pp 1−91.

Cernik, M.; Borkovec, M.; Westall, J. C. Regularized Least-Squares Methods for the Calculation of Discrete and Continuous Affinity Distributions for Heterogeneous Sorbents. *Environ. Sci. Technol.* **1995,** *29*, 413−425.

ChemPlus: Extension for HyperChem; Hypercube: Ontario, Canada, 1993; p 1.

Cole, R. J.; Cox, R. H. The Aflatoxins. In *Handbook of Toxic Fungal Metabolites*; Academic Press: New York, 1981; pp 11−66.

Dewar, M. J. S.; Zoebisch, E. G.; Healy, E. F.; Stewart, J. J. P. AM1: A New General Purpose Quantum Mechanical Molecular Model. *J. Am. Chem. Soc.* **1985**, *107*, 3902−3909.

Dyal, R. S.; Hendricks, C. B. Total Surface of Clays in Polar Liquids, as a Characteristic Index. *Soil Sci.* **1950**, *69*, 421−432.

Emsley, J. *The Elements*, 2nd ed.; Clarendon Press: Oxford, U.K., 1991; p 1.

Fischer, R. B.; Peters, D. G. *Chemical Equilibrium*; W. B. Saudners: Philadelphia, PA, 1970; p 1.

Gatta, G. D. Direct Determination of Adsorption Heats. *Thermochim. Acta* **1985**, *96*, 349−363.

Ghose, A. K.; Pritchett, A.; Crippen, G. M. Atomic Physicochemical Parameters for Three Dimensional Structure Directed Quantitative Structure-Activity Relationships III: Modeling Hydrophobic Interactions. *J. Comput. Chem.* **1988**, *9*, 80−90.

Giles, C. H.; MacEwan, T. H.; Nakhwa, S. N.; Smith, D. Studies in Adsorption. Part XI. A System of Classification of Solution Adsorption Isotherms, and its Use in Diagnosis of Adsorption Mechanisms and in Measurement of Specific Areas of Solids. *J. Chem. Soc.* **1960**, 3973−3993.

Giles, C. H.; Smith, D.; Huitson, A. A General Treatment and Classification of the Solute Adsorption Isotherm I. Theoretical. *J. Colloid Interface Sci.* **1974a**, *47*, 755−765.

Giles, C. H.; D'Silva, A. P.; Easton, I. A. A General Treatment and Classification of the Solute Adsorption Isotherm Part II. Experimental Interpretation. *J. Colloid Interface Sci.* **1974b**, *47*, 766−778.

Goto, T.; Matsui, M.; Kitsuwa, T. Determination of Aflatoxins by Capillary Column Gas Chromatography. *J. Chromatogr.* **1988**, *447*, 410−414.

Gray, M. J.; Mebane, R. C.; Womack, H. N.; Rybolt, T. R. Molecular Mechanics and Molecular Cross-Sectional Areas: A Comparison with Molecules Adsorbed on Solid Surfaces. *J. Colloid Interface Sci.* **1995**, *170*, 98−101.

Gu, B.; Schmitt, J.; Chen, Z.; Liang, L.; McCarthy, J. F. Adsorption and Desorption of Natural Organic Matter on Iron Oxide: Mechanisms and Models. *Environ. Sci. Technol.* **1994**, *28*, 38−46.

Harvey, R. B.; Phillips, T. D.; Ellis, J. A.; Kubena, L. F.; Huff, W. E.; Peterson, H. D. Effects of Aflatoxin M_1 Residues in Milk by Addition of Hydrated Sodium Calcium Aluminosilicate to Aflatoxin Contaminated Diets of Dairy Cows. *Am. J. Vet. Res.* **1991**, *52*, 1556−1559.

HyperChem: Computational Chemistry; Hypercube, Inc.: Ontario, Canada, 1994, pp 1−285.

Kinniburgh, D. G. General Purpose Adsorption Isotherms. *Environ. Sci. Technol.* **1986**, *20*, 895−904.

Klein, W.; Kordel, W.; Weib, M.; Poremski, H. J. Updating of the OECD Test Guideline 107 "Partition coefficient *N*-octanol/water": OECD Laboratory Intercomparison test on the HPLC Method. *Chemosphere* **1988**, *17*, 361−386.

Langmuir, I. The Constitution and Fundamental Properties of Solids and Liquids. *J. Am. Chem. Soc.* **1916**, *38*, 2221−2294.

Meylan, W. M.; Howard, P. H.; Boethling, R. S. Improved Method for Estimating Water Solubility from Octanol/Water Partition Coefficient. *Environ. Toxicol. Chem.* **1996**, *15*, 100−106.

Mortland, M. M.; Kemper, W. D. Specific Surface. In *Methods of Soil Analysis Part 1: Physical and Mineralogical Properties, Including Statistics of Measurement and Sampling*; Black, C. A., Ed.; American Society of Agronomy: Madison, WI, 1965; pp 532−544.

Nakamoto, K. *Infrared Spectra of Inorganic and Coordinarion Compounds;* Wiley: New York, 1963.

Phillips, T. D.; Kubena, L. F.; Harvey, R. B.; Taylor, D. R.; Heidelbaugh, N. D. Hydrated Sodium Calcium Aluminosilicate: A High Affinity Sorbent for Aflatoxin. *Poult. Sci.* **1988**, *67*, 243−247.

Phillips, T. D.; Sarr, A. B.; Grant, P. G. Selective Chemisorption and Detoxification of Aflatoxins by Phyllosilicate Clay. *Nat. Toxins* **1995**, *3*, 204−213.

Sarr, A. B. Evaluation of Innovative Methods for the Detection and Detoxification of Aflatoxin. Ph.D. Dissertation, Texas A&M University, 1992.

Smith, E. E.; Phillips, T. D.; Ellis, J. A.; Harvey, R. B.; Kubena, L. F.; Thompson, J.; Newton, G. Dietary Hydrated Sodium Calcium Aluminosilicate Reduction of Aflatoxin M_1 Residue in Diary Goat Milk and Effects on Milk Production and Components. *J. Anim. Sci.* **1994**, *72*, 677−682.

Shepherd, E. C.; Phillips, T. D.; Heidelbaugh, N. D.; Hayes, A. W. High Pressure Liquid Chromatographic Determination of Aflatoxins by Using Radial Compression Separation. *J. Assoc. Off. Anal. Chem.* **1982**, *65*, 665−671.

Stumm W.; Sigg, L.; Sulzberger, B. *Chemistry of the Solid-Water Interface*; Wiley: New York, 1992; p 1.

Vellarkad, N.; Viswanadhan, V. N.; Ghose, A. K.; Revankar, G. N.; Robins, R. K. Atomic Physiochemical Parameters for Three Dimensional Structure Directed Quantitative Structure-Activity Relationships. 4. Additional Parameters for Hydrophobic and Dispersive Interactions and Their Application for an Automated Superposition of Certain Naturally Occurring Nucleoside Antibiotics. *J. Chem. Inf. Comput. Sci.* **1989**, *29*, 163−172.

Wogan, G. N.; Newberne, P. M. Dose-response Characteristics of Aflatoxin B_1 Carcinogenesis in Rats. *Cancer Res.* **1967**, *27*, 2370−2376.

Received for review July 15, 1997. Accepted October 30, 1997.[⊗] This study was supported by funding from the Texas Agricultural Experiment Station Project H-6215 and ATP Project 999902-004.

JF970604V

[⊗] Abstract published in *Advance ACS Abstracts,* December 15, 1997.